Carrageenan from *Chondracanthus Chamissoi* Algae: Extraction process and experimental evaluation as green corrosion inhibitor for P22 steel in HCl

N. Zavaleta-Gutierrez,[1]* L. Alvarado-Loyola,[1] L. Angelats-Silva,[2] N. Ñique-Gutierrez[3] and G. Duffó[4]

[1]*Metallurgical Engineering Department, Trujillo National University, Av. Juan Pablo II s/n, Trujillo 13011, Perú*

[2]*Multidisciplinary Research Laboratory, Antenor Orrego Private University, Trujillo 13008, Perú*

[3]*Materials Engineering Department, Trujillo National University, Av. Juan Pablo II s/n, Trujillo 13011, Perú*

[4]*National Commission of Atomic Energy, Corrosion Department, Av. Gral. Paz 1499, 1650 San Martín, National University of San Martín and CONICET, Buenos Aires, Argentina*

**E-mail: nzavaleta@unitru.edu.pe*

Abstract

In this study, the extraction yield of carrageenan from the algae *Chondracanthus Chamissoi* and its efficiency as an ecological corrosion inhibitor for P22 steel in 1 M HCl at 65°C were evaluated. The extraction of carrageenan from the algae *Chondracanthus chamissoi* was carried out in cold water at 25°C (CC) and hot water at 80°C (HC), with different degreasing stages prior to the extraction (0, 1 and 2 stages). The codes of the six samples of carrageenan obtained were selected in terms of the production temperature and degreasing stages as: CC-0, CC-1, CC-2, HC-0, HC-1 and HC-2. All the carrageenan samples were characterized using: Fourier transform infrared spectroscopy, X-ray diffraction, scanning electron microscopy and energy dispersive spectrum. The CC shows crystallinity and is mainly composed of κ-carrageenan in the presence of KCl, NaCl and $K_3Na(SO_4)_2$; while the degreasing stages reduce the content of KCl and NaCl. The HC presents an amorphous structure composed of κ/ι carrageenans. The highest carrageenan extraction yielded in cold water was 21.43%, without the degreasing stage (CC-0); while, the highest carrageenan extraction yielded in hot water was 28.96% with 2 degreasing stages (HC-2). The inhibition performance was investigated using gravimetric analysis, potentiodynamic polarization, linear polarization resistance, electrochemical impedance spectroscopy and electrochemical frequency modulation. The experimental results demonstrated that all six carrageenan inhibitors act as good corrosion inhibitors for P22 steel in 1 M HCl at 65°C. However, the CC-0 presented the maximum corrosion inhibition efficiency (IE_c) of 85.53% (EIS technique). In the HC, the degrease does not significantly affect IE_c, allows to obtain 82.56% without degrease (EIS technique). Based on the results obtained, the extraction CC-0 and HC-0 in the same extraction process, allows to obtain a semi-refined, economical carrageenan, with a total carrageenan yield of 45.91%, and with a high IE_c.

Received: June 12, 2022. Published: July 23, 2022 doi: 10.17675/2305-6894-2022-11-3-7

Keywords: *ecological corrosion inhibitor, carrageenan, Chondracanthus chamissoi.*

1. Introduction

Corrosion is a spontaneous process that is generated through the chemical or electrochemical interaction of metallic materials with their environment, transforming them into their most stable forms such as oxides, sulfides, sulfates, *etc.* Economic losses as a consequence of corrosion range between 2.4 and 4.5% of the GNP (Gross National Product) of industrialized countries such as the USA, China, India, *etc.* [1]. Low alloy Cr–Mo steels are widely used in tubular components in thermoelectric and petrochemical plants, due to their good resistance to creep. During the operation of these plants, there is a progressive growth of corrosion products inside the tubes, that often have to be cleaned for normal operation. Chemical cleaning, especially with HCl, is the most used technique in these tubular components [2]. However, HCl is very corrosive so it must be used with additions of corrosion inhibitor (CI) to avoid the corrosive attack of the acid on the steel. The corrosion inhibitors (CIs) are considered to function by adsorption on the surface of steel, resulting in a protective layer on the surface [3, 4]. The adsorption is achieved by chemical interactions between the unshared electrons of the S, O, P and N atoms, present in the CI, with the empty iron orbitals on the surface of the steel [5, 6]. Various inorganic and synthetic organic compounds are used commercially as CI [7]. These inhibitors are effective, but also expensive and toxic in nature. The demand for low-cost, non-toxic and biodegradable corrosion inhibitors has shifted the focus of some researchers towards natural plant extracts, also known as "green corrosion inhibitors" [8, 9].

In the last decade there have been many studies on the use of natural gums as eco-friendly CIs for metals and alloys. Almond gum (AG) was evaluated as a green corrosion inhibitor in 1 M HCl on mild steel (MS), using the gravimetric technique in the temperature range of 30 to 60°C [10]. It was reported that its IE_c increased with increasing concentration and temperature, giving an IE_c of 96.37% at 60°C with a dosage of 300 ppm of AG. The adsorption of AG on MS followed Langmuir adsorption isotherm [10]. Locust bean gum (LBG) was found to be a good CI of Q235 steel in 0.5 M H_2SO_4. The results of potentiodynamic polarization test showed that, when the concentration of LBG is 5 mM at 25°C, the IE_c is 89.8%. The adsorption of LBG on Q235 steel was consistent with Langmuir adsorption isotherm [11]. Shamsheera *et al*. investigated the anticorrosive effect of guar gum (GG) on MS in 0.5 N HCl by weight loss and electrochemical methods in the range of 30 to 50°C. The maximum *IE* of 92.74% at 25°C was obtained with 800 ppm of GG (EIS technique). Adsorption studies revealed that GG adsorbed on the MS surface in accordance with Langmuir adsorption isotherm [12]. Mobin *et al*. [13], reported that *Boswellia serrata* gum (BSG) exhibits an IE_c of 95.49% on MS in 1 M HCl at 30°C at 500 ppm concentration using potentiodynamic polarization technique. The process of adsorption of BSG constituents on MS followed Langmuir adsorption isotherm and the thermodynamic and

activation parameters determined that the BSG constituents interact with the surface of MS via a mechanism of physisorption and chemisorption [13]. In another study conducted by Mobin *et al*. [14], they tested tragacanth gum as a CI on MS in 1 M HCl, using weight loss, electrochemical impedance and potentiodynamic polarization techniques, in the temperature range from 30°C to 60°C. The gum was reported to have an IE_c of 96.3% for a concentration of 500 ppm at 60°C. The IE_c increases with gum concentration and temperature. The adsorption mechanism was of the physisorption type [14]. Biswas *et al*. [15], studied xanthan gum (XG) as a CI on MS in 15% HCl using gravimetric technique. The experimental results show an IE_c of 90.8% for a concentration of 500 ppm at 25°C [15]. However, studies conducted by Mobin and Rizvi [16], with the XG on MS in 1 M HCl, reported only a maximum IE_c of 74.24% at 30°C at a comparatively higher concentration of 1000 ppm. In both cases the XG was purchased in pure form, but from different manufacturers. The anticorrosive properties of gum arabic for steel and aluminum in 2 M H_2SO_4, were determined by weight loss and thermometric techniques, in the temperature range from 30°C to 60°C [17]. With a dosage of 500 ppm of gum arabic, an IE_c of 79.69% was observed at 30°C for aluminum; while for steel the IE_c was 37.88% at 60°C. The adsorption of gum arabic on steel and aluminum obeyed the Temkin adsorption isotherm and chemical adsorption for steel and physical adsorption for aluminum were reported [17]. These gums are natural polymers made up of polysaccharides enriched with O and N atoms that serve as adsorption sites, forming a film that isolates the metal surface from the corrosive environment. Efforts are ongoing to increase information on environmentally friendly polymeric corrosion inhibitors.

Chondracanthus chamissoi is a red benthic marine alga that is distributed from Paita, Peru to Ancud, Chile. This alga contains two types of carrageenan, κ-carrageenan and ι-carrageenan, which are extracted through different processes [18]. Carrageenans are sulfated polysaccharide that contains many electron – rich heteroatoms (O and S) and hydroxyl functional groups. This composition shows the potential of this molecule as an efficient inhibitor in aggressive acidic media. In addition, carrageenan is easily obtained with inexpensive processes and with excellent yield. These properties indicate the economic potential of carrageenan in industry for its use as a corrosion inhibitor to protect metals from acid corrosion. P22 is a low-alloy steel, standardized 2.25% Cr–1% Mo and widely used as a tubular component in conventional thermoelectric plants. [19]. The present study shows the form of extraction and the anticorrosive property of the carrageenan obtained from *Chondracanthus chamissoi* for use on P22 steel in 1 M HCl at 65°C. The relevance of this study was to obtain an inexpensive semi-refined carrageenan with high extraction yield and high corrosion inhibition efficiency. For this purpose, only the degreasing stage of the algae prior to the extraction of the carrageenans at 25°C and 80°C is considered. The carrageenans obtained were characterized by Fourier transform infrared spectroscopy (FTIR), X-ray diffraction (XRD) and scanning electron microscopy – Energy Dispersive Spectroscopy (SEM-EDS). The inhibition properties of carrageenans were evaluated, using five techniques: gravimetric (Weight loss, WL), potentiodynamic polarization (PDP), linear

polarization resistance (LPR), electrochemical impedance spectroscopy (EIS) and electrochemical frequency modulation (EFM).

2. Materials and Methods

2.1. Materials

The *Chondracanthus chamissoi* algae was collected in the coastal area of the city of Trujillo, Peru. The corrosion tests were carried out with working electrodes manufactured from a seamless tube of P22 steel used in the pipelines of conventional thermoelectric plants. The composition of the P22 steel in % weight was 0.115% C; 0.46% Mn; 0.23% Si; 0.005% S; 0.009% P; 1.96% Cr; 0.85% Mo, and Fe balance, obtained by the optical emission spectrometry (OES) method.

2.2. Extraction of carrageenan

Carrageenans were obtained from the alga *Chondracanthus chamissoi* by the method proposed by Yu *et al*. [20], with certain modifications to obtain a low-cost carrageenan for use as a corrosion inhibitor. The algae were washed and dried in the environment for 15 days. Subsequently the algae were degreased with 96% ethanol for 3 h at 80℃, in several stages. In this part of the study, the effect of degreasing was evaluated and up to two degreasing stages were considered. With the algae without and with the degreasing process, the first extraction was carried out, in double distilled water at 25±2℃ in two stages of 3 h each one. The solution containing the carrageenan from this stage was obtained by vacuum filtration, subsequently evaporated in an oven at 100°C and the cold carrageenan (CC) obtained was pulverized. With the residue from the cold extraction, the extraction was carried out hot condition, in double distilled water at 80±2°C, in two stages of 3 h each them. The procedure was similar to that carried out with CC, that is, the solution containing carrageenan was filtered, evaporated in an oven at 100°C, pulverized and named as hot carrageenan (HC). As the process was continuous, CC and HC were obtained without degreasing (CC-0, HC-0), CC and HC with 1 degreasing process (CC-1, HC-1), and CC and HC with 2 degreasing process (CC-2, HC-2). The extraction procedure is shown in detail in Figure 1.

2.3. Characterization of carrageenans

All carrageenans were characterized by FTIR (Thermo Scientific Nicolet iS50), XRD (Bruker D8 Advance Eco) and SEM-EDS (Tescan Vega 3 LMU).

2.4. Gravimetric analysis

Thin sheet samples of P22 steel with exposed area between 14 to 15 cm^2 were used. The samples were polished to 1000 grit, washed in distilled water, acetone and dried with warm air. The area was calculated and the weight of each sample was recorded using an analytical balance (±0.1 mg). Subsequently, the samples were immersed in 350 ml of the 1 M HCl

solution with 1.5 g·L^{-1} carrageenan (concentration determined in preliminary tests) for 3 h at 65°C. After exposure, the samples were rinsed with water and cleaned with a bristle brush; followed by a rinse with distilled water and acetone. The samples were dried in warm air and the weight was recorded. All tests were carried out in at least by triplicate. To calculate the corrosion rate $\left(V_{\text{corr}}^{\text{WL}}\right)$, in mm/year, equation (1) was used, which corresponds to uniform corrosion.

$$V_{\text{corr}}^{\text{WL}}\left[\frac{\text{mm}}{\text{year}}\right]=8.76\cdot10^{4}\left[\frac{m_1-m_2}{A\cdot t}\right]\left[\frac{1}{\rho}\right] \tag{1}$$

where, m_1 and m_2 are the masses (g) of the steel sample before and after immersion in the test solution, respectively; A is the exposed area of the sample (cm^2); t is the immersion time (h); and ρ is the density of the steel (7.86 g·cm^{-3}). The percentage of inhibition efficiencies (%IE_{WL}) was calculated using the equation (2):

$$\%IE_{\text{WL}}=\frac{V_{\text{corr,0}}^{\text{WL}}-V_{\text{corr,inh}}^{\text{WL}}}{V_{\text{corr,0}}^{\text{WL}}}\cdot100 \tag{2}$$

where, $V_{\text{corr,0}}^{\text{WL}}$ and $V_{\text{corr,inh}}^{\text{WL}}$ are the $V_{\text{corr}}^{\text{WL}}$ of steel in the absence and presence of carrageenan, respectively.

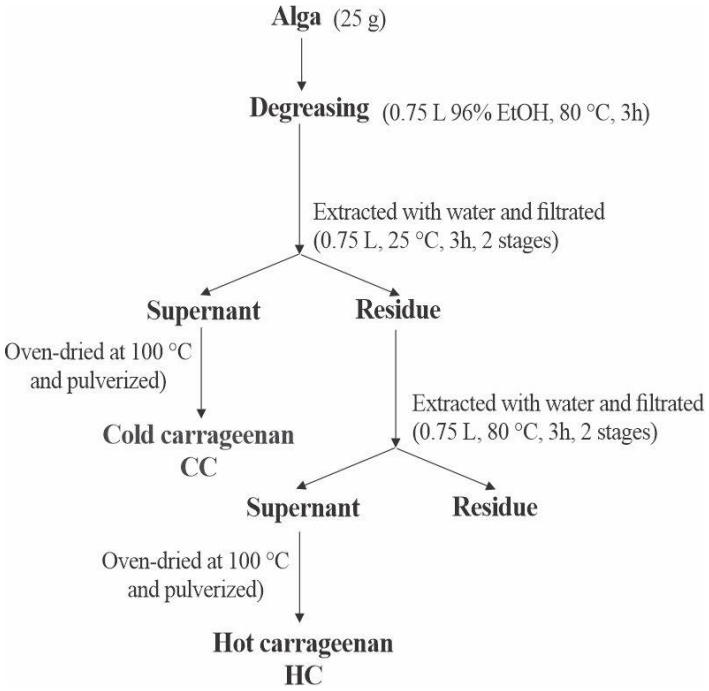

Figure 1. Chart of carrageenan extraction from the alga *Chondracanthus chamissoi*.

2.5. Electrochemical analysis

To perform the electrochemical test, a standard three-electrode cell was employed with a cylindrical P22 steel working electrode (3 to 3.5 cm^2), a saturated calomel reference

electrode and a graphite rod as counter electrode. The 1 M HCl solution was prepared by dissolving the 36% HCl with double distilled water, to which 1.5 $g \cdot L^{-1}$ of carrageenan was added. All tests were performed at least by triplicate using a Gamry Reference 3000 potentiostat. Prior to the tests, the working electrode was kept for 30 min in the acid solutions before the start of the measurements to achieve a quasi-stationary open circuit potential (E_{OCP}). The potentiodynamic polarization (PDP) curves were obtained in the range of ±250 mV *vs.* E_{OCP}, at a scanning rate of 0.5 $mV \cdot s^{-1}$. Using the Tafel method, the corrosion current density $\left(i_{corr}^{PDP}\right)$ and the anodic and cathodic Tafel slopes (β_a and β_c) of each test were obtained from the PDP curves. The inhibition efficiency (%IE_{PDP}) of carrageenan was calculated from equation (3):

$$\%IE_{PDP} = \frac{i_{corr,0}^{PDP} - i_{corr,inh}^{PDP}}{i_{corr,0}^{PDP}} \cdot 100 \quad (3)$$

where, $i_{corr,0}^{PDP}$ and $i_{corr,inh}^{PDP}$ are the corrosion current densities without and in the presence of carrageenan, respectively. The linear polarization resistance (LPR) experiments were carried out in the range of ±20 mV *vs.* E_{OCP}, at a scanning rate of 0.1 mV/s, and the value of R_p was obtained from the slope of the curve *E vs. i*, in the vicinity of the E_{OCP}, using a Gamry's DC105 software. The inhibition efficiency (%IE_{LPR}) of carrageenan was calculated from equation (4):

$$\%IE_{LPR} = \frac{R_{p,inh} - R_{p,0}}{R_{p,inh}} \cdot 100 \quad (4)$$

where, $R_{p,0}$ and $R_{p,inh}$ are the polarization resistance values in the absence and presence of carrageenan, respectively. The electrochemical frequency modulation (EFM) measurements were performed applying a potential perturbation signal with an amplitude of 10 mV with two sine waves of 2 and 5 Hz. With the intermodulation spectra and using the EFM 140 software, the corrosion current density $\left(i_{corr}^{EFM}\right)$, the Tafel slopes ($\beta_c$ and β_a) and the causality factors (*CF*2 and *CF*3) [21] were obtained. The inhibition efficiency (%IE_{EFM}) of carragenan was calculated according to equation (5):

$$\%IE_{EFM} = \frac{i_{corr,0}^{EFM} - i_{corr,inh}^{EFM}}{i_{corr,0}^{EFM}} \cdot 100 \quad (5)$$

where, $i_{corr,0}^{EFM}$ and $i_{corr,inh}^{EFM}$ are the values of i_{corr}^{EFM} in the absence and presence of carrageenan, respectively. Electrochemical impedance spectroscopy (EIS) tests were carried out using an AC signals of amplitude 10 mV with respect to E_{OCP} in the frequency range 10 kHz to 0.10 Hz. Using Gamry's EIS3000 software, the impedance data obtained was fitted to a modified Randles circuit with a constant phase element, obtaining the solution resistance

(R_s), charge transfer resistance (R_{ct}) and the capacitance of the electrical double layer (C_{dl}). The inhibition efficiency (%IE_{EIS}) of carrageenan was calculated according to equation (6):

$$\%IE_{EIS} = \frac{R_{ct,inh} - R_{ct,0}}{R_{ct,inh}} \cdot 100 \quad (6)$$

where, $R_{ct,0}$ and $R_{ct,inh}$ are the charge transfer resistances without and in the presence of carrageenan, respectively.

3. Results and Discussion

3.1. Carrageenan obtained at 25°C with different degrease stages

3.1.1. Cold carrageenan yield

The extraction yield (*EY*) of the carrageenan, is the percentage of the weight of the carrageenan obtained with respect to the weight of the dried *Chondracanthus chamissoi* algae. Table 1 shows the statistical results of the analysis of variance (ANOVA) and the results of Dunnett's multiple comparison test of the cold carrageenan extraction yield (EY_{CC}), obtained as a function of the degreasing stages applied in the extraction tests. As observed, the 95% confidence interval ($CI_{95\%}$) for each mean EY_{CC} as a function of the degrease stages do not overlap, which indicates that they are significantly different. Likewise, Dunnett's method generates $CI_{95\%}$ for the differences between the yield means obtained with the degreasing stages (1 and 2) and the yield mean without degrease (control group, 0). These $CI_{95\%}$ determine two significant aspects, first they do not contain zero, which indicates a significant difference between the yield obtained by applying 1 and 2 degreasing stages; second, the $CI_{95\%}$ contains only negative numbers; inferring that degrease generates a lower EY_{CC}. The *p*-values of the *t*-Student test are less than 0.05, establishing a statistically significant difference between the means of the EY_{CC} without and with degrease stages, with a confidence level of 97.31%.

Table 1. Statistical results of the ANOVA and Dunnett's multiple comparison tests for the extraction yield of CC with different degreasing stages.

Degreasing stages	***N***	**Mean**	**Std Deviation**	***CI*$_{95\%}$**
0	12	21.434	0.792	(20.986–21.882)
1	9	19.704	0.790	(19.187–20.222)
2	10	17.691	0.681	(17.200–18.182)

Level difference	**Mean difference**	**Std Error of difference**	***CI*$_{95\%}$**	***t*-value**	***p*-value**
1–0	–1.730	0.334	(–2.510; –0.949)	–5.18	0.000
2–0	–3.743	0.324	(–4.501; –2.985)	–11.54	0.000

3.1.2. Cold carrageenan characterization

The X-ray diffraction pattern of the CC, obtained with different degreasing stages are shown in Figure 2. The characteristic peaks in the diffraction pattern correspond to KCl, NaCl and $K_3Na(SO_4)_2$. In the CC obtained without degrease, the content KCl and NaCl is higher; while, in the CC obtained with one and two degreasing, $K_3Na(SO_4)_2$ predominates. During degreasing, a large part of the KCl and NaCl are removed, which probably influenced the lower EY of the CC obtained with degrease, see Table 1.

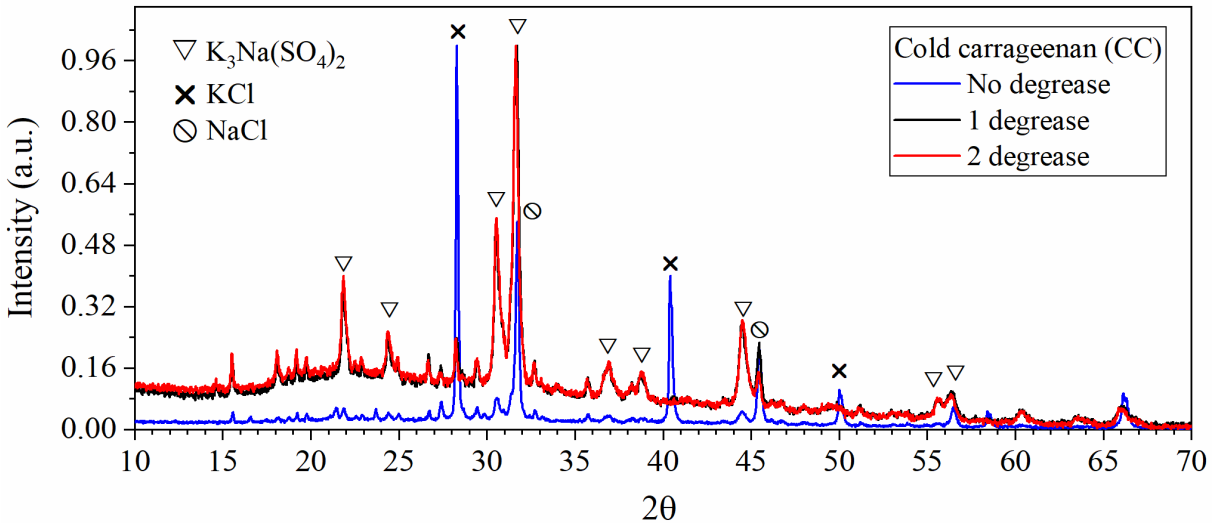

Figure 2. X-ray diffraction pattern of carrageenans obtained at 25°C with different degreasing stage.

Figure 3 shows the SEM image of the CC without degreasing together with the EDS spectra corresponding to the total mapping of the CC analyzed. Semi-quantitative analysis confirmed the presence of Cl, K, Na, S and O; which are the main elements in the phases identified by XRD. The spot EDS spectra carried out on the CC sample showed semi-quantitative compositions very similar to those carry out on the total sample. The presence of Mg and P were in smaller quantities.

Figure 4 shows the FTIR spectrums obtained from the CC with different degreasing stages. A broad band is observed at 1230 cm^{-1} that is characteristic of the S=O bonds of the sulfate esters of the carrageenans [22]. The bands at 1072 cm^{-1} and 930 cm^{-1}, both correspond to the C–O bond of 3,6-anhydrogalactose [22]. The region around 800–850 cm^{-1} was used to identify the position of the sulfate group in carrageenan. The broad bands at 845 and 805 cm^{-1} suggested the presence of C–O–SO_4 bonds on C_4 of galactose and of C–O–SO_4 bonds on C_2 of 3,6-anhydrogalactose, respectively [22, 23]. Therefore, the structural character of CC is a mixture of κ-carrageenan, with a low content of ι-carrageenan [22, 23]. The characteristic bands at 614 cm^{-1}, 1100 cm^{-1} and 1191 cm^{-1} correspond to $K_3Na(SO_4)_2$ [24]; which, as can be seen, the peaks are greater with the degreasing applied, probably due to its greater presence of this phase in carrageenan.

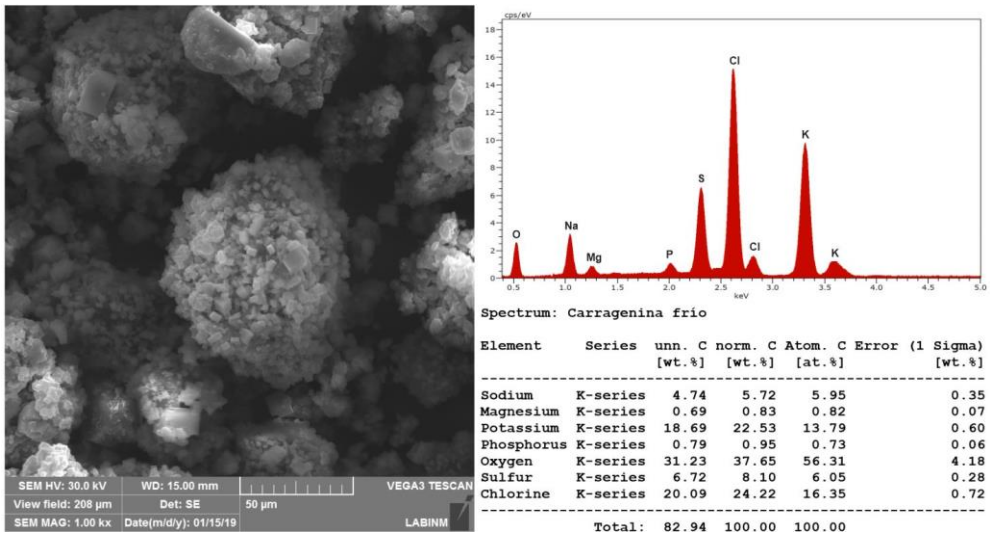

Spectrum: Carragenina frío

Element	Series	unn. C [wt.%]	norm. C [wt.%]	Atom. C [at.%]	Error (1 Sigma) [wt.%]
Sodium	K-series	4.74	5.72	5.95	0.35
Magnesium	K-series	0.69	0.83	0.82	0.07
Potassium	K-series	18.69	22.53	13.79	0.60
Phosphorus	K-series	0.79	0.95	0.73	0.06
Oxygen	K-series	31.23	37.65	56.31	4.18
Sulfur	K-series	6.72	8.10	6.05	0.28
Chlorine	K-series	20.09	24.22	16.35	0.72
	Total:	82.94	100.00	100.00	

Figure 3. SEM image and total EDS spectrum of carrageenan obtained at 25°C without degrease (CC-0).

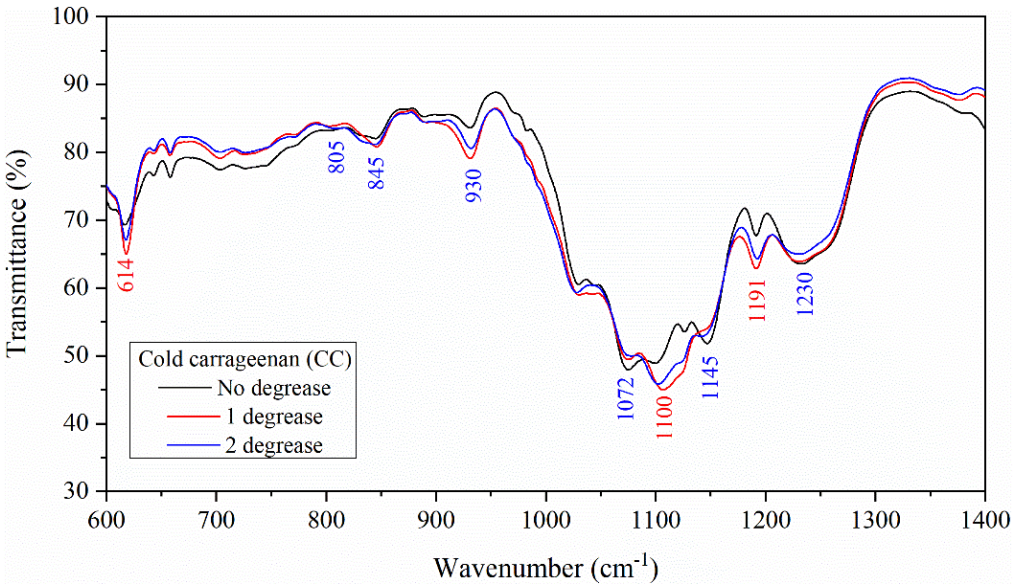

Figure 4. FTIR spectrums of carrageenan obtained 25°C with different degreasing stages.

3.1.3. Corrosion inhibition efficiency of cold carrageenan

The CC with different degreasing stages were evaluated for their corrosion inhibiting effect on P22 steel in 1 M HCl at 65°C, using five techniques: gravimetric (WL), potentiodynamic polarization (PDP), linear polarization resistance (LPR), electrochemical frequency modulation (EFM) and electrochemical impedance spectroscopy (EIS).

Gravimetric measurements

In these tests, the mass loss of the metal of known area, exposed to the corrosive medium for a predetermined period of time, is measured. Table 2 shows the corrosion rate $\left(V_{\text{corr}}^{\text{WL}}\right)$ of

P22 steel in 1 M HCl at 65°C, without and with 1.5 g·L^{-1} of CC obtained with different degreasing stages, after 3 hours of immersion. It is evident that the three types of CC have a good inhibition efficiency (%IE_{WL}). The presence of oxygen and sulfur heteroatoms in carrageenan can be responsible for the adsorption of the inhibitor on the steel surface. However, CC-0 presented better inhibition efficiency than CC-1 and CC-2, which was confirmed by the $CI_{95\%}$ of the inhibition efficiency means (IE_{WL}) of the three HC, obtained with the ANOVA, Table 2. This can be attributed to the enhanced adsorption of carrageenan in the presence of KCl and NaCl because of the synergistic effect of chloride ions. Several works have reported the synergistic effect between halide ions and CIs, due to the fact that the halide anion enhances the corrosion inhibition mechanism carried out by an organic compound [25].

Table 2. Weight loss results of P22 steel in 1 M HCl at 65°C, in the absence and presence of 1.5 g·L^{-1} of CC with different degreasing stages.

Inhibitor	V_{corr}^{WL} (mm·year^{-1})	%IE_{WL}	$CI_{95\%}$
Blank	26.97±0.43	Blank	Blank
CC-0	3.20±0.13	88.15±0.49	(87.61; 88.69)
CC-1	3.56±0.10	86.79±0.37	(86.25; 87.33)
CC-2	3.63±0.06	86.55±0.24	(86.01; 87.09)

Potentiodynamic polarization measurements

PDP measurements were used to distinguish the effects of different carrageenan inhibitors (CC-0, CC-1 and CC-2), on the anodic and cathodic corrosion reactions. Figure 5 shows PDP curves for P22 steel in 1.0 M HCl at 65°C, in the absence and presence of CC at the concentration of 1.5 g·L^{-1}. The PDP parameters of the test performed are shown in Table 3. It is clear that the addition of carrageenan molecules into the acid media promotes the remarkable lowering in both anodic and cathodic current densities over the entire potential range, which should be owing to the formation of protective films of inhibitors on steel surface. According to Table 3, the three CC show good IE_{PDP} for P22 steel in 1 M HCl at 65°C; with 1.5 g·L^{-1} of CC-0, the i_{corr}^{PDP} value decreased drastically from 2.058 mA·cm^{-2} to 0.182 mA·cm^{-2}, with an inhibition efficiency to about 91%. This clearly shows that CC-0 is a high-efficiency corrosion inhibitor for P22 steel at 65°C, which was statistically confirmed in the ANOVA analysis.

The change of the values of E_{corr} exceeding 85 mV is usually considered to correspond to a cathodic type or otherwise an anodic type corrosion inhibitor. The maximum change of E_{corr} was about 14 mV, showing that all CC inhibitors tested are in the category of the mixed type inhibitors. In addition, the values of E_{corr} in the presence of the CC were shifted toward a more positive direction. The results suggest that carrageenan is preferentially adsorbed on

the anodic sites and mainly prevents the dissolution of P22 steel. In Table 3, It can be seen that the inhibitor efficiencies of three CCs are in the order CC-0>CC-1≈CC-2, which is consistent with the results obtained from gravimetric measurements.

Table 3. Potentiodynamic polarization parameters for corrosion of P22 steel in 1 M HCl at 65°C without and with 1.5 g·L^{-1} of CC with different degreasing stages.

Inhibitor	i_{corr}^{PDP} (μA·cm^{-2})	$-E_{corr}$ (mV *vs.* SCE)	β_a (mV·dec^{-1})	β_c (mV·dec^{-1})	IE_{PDP} (%)	$CI_{95\%}$
Blank	2058.2±142.2	420.3±0.8	65.2±2.6	127.6±2.3	Blank	Blank
CC-0	182.1±16.5	416.9±1.0	28.5±0.9	137.3±6.9	91.1±0.7	(90.1; 92.0)
CC-1	327.7±13.1	415.7±0.3	32.5±0.8	187.9±4.2	84.1±0.6	(83.0; 85.2)
CC-2	330.1±21.2	406.2±0.4	23.4±1.2	181.3±3.9	84.0±1.0	(82.9; 85.0)

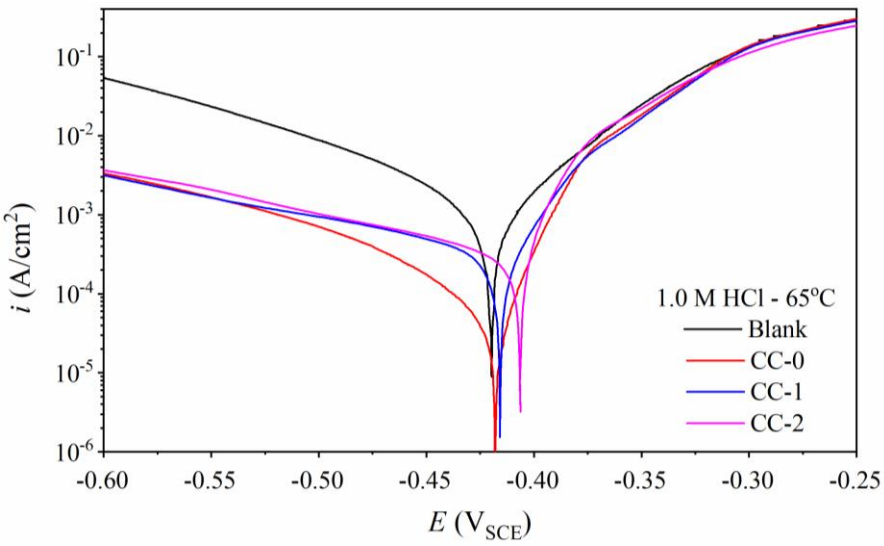

Figure 5. Effect of the type of CC, with a concentration of 1.5 g·L^{-1}, on the potentiodynamic curves of P22 steel in 1 M HCl at 65°C.

Linear polarization resistance measurements

LPR plots for P22 steel in 1 M HCl without and with 1.5 g·L^{-1} of CC obtained with different degreasing stages are shown in Figure 6. A polarizing voltage of 20 mV was chosen because it is well within the range where the relationship between i_{corr} and E is linear. Polarization resistance (R_p) values increase with the CC as shown in Table 4. This increase indicates that the carrageenan molecules are adsorbed on the surface of the P22 steel, which hinders the charge transfer process in the corrosive process, decreasing $V_{corr}^{R_p}$ and increasing IE_{R_p}. Moreover, CC-0 had the highest inhibition efficiency $\left(\%IE_{R_p} = 82.8\right)$ compared to CC-1 and CC-2.

Table 4. Results of polarization resistance tests for corrosion of P22 steel in 1 M HCl at 65°C without and with 1.5 g·L^{-1} of CC with different degreasing stages.

Inhibitor	R_p (Ω·cm^2)	V_{corr}^{Rp} (mm·year^{-1})	IE_{Rp} (%)	$CI_{95\%}$
Blank	14.87±0.51	12.87±0.44	Blank	Blank
CC-0	86.58±3.05	2.55±0.09	82.8±0.6	(82.1; 83.5)
CC-1	73.96±2.30	3.08±0.10	79.9±0.6	(79.2; 80.6)
CC-2	74.47±4.16	2.80±0.16	80.0±1.1	(79.3; 80.7)

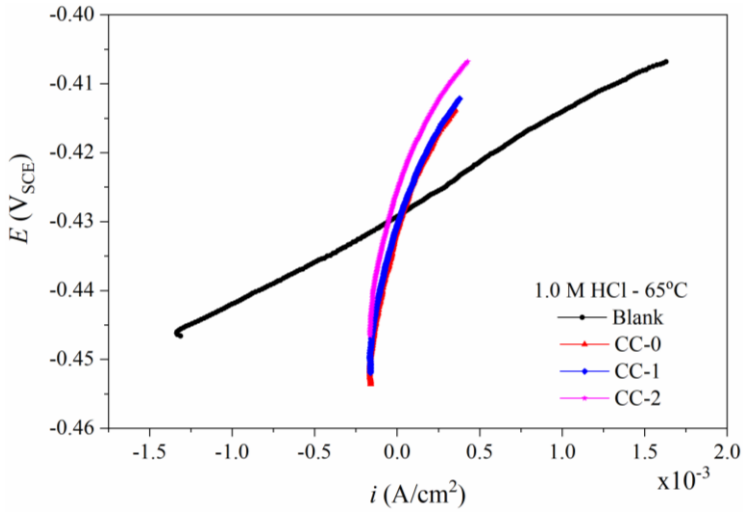

Figure 6. Effect of the type of CC, with a concentration of 1.5 g·L^{-1}, on the linear polarization resistance curves of P22 steel in 1 M HCl at 65°C.

Electrochemical frequency modulation measurements

It is a non-destructive technique, which allows obtaining the corrosion current density and the Tafel slopes in a straightforward manner. The EFM intermodulation spectra for the blank and CC are found (Figure 7), and the current density peaks in these spectra are utilized to measure the EFM kinetic parameters [21, 26], shown in Table 5. It is evident from the intermodulation spectra shown in Figure 6, that the corrosion peak current density is lower in presence of the CC. The results presented in Table 5 indicate that the addition of 1.5 g·L^{-1} of CC to the 1 M HCl solution at 65°C decreases the i_{corr}^{EFM} of the P22 steel, which suggests that the three types of CC, inhibit the corrosion of P22 steel through its adsorption. The CC-0 generates the highest inhibition efficiency (%IE_{EFM} = 83.0) compared to CC-1 and CC-2; this is statistically confirmed in the ANOVA analysis realized. The degreasing stage reduces the anticorrosive power of the CC; and this is probably due to the elimination of KCl and NaCl. Several works have reported that Cl^- ions enhance the adsorption of organic inhibitor on the metal surface [27, 28]. The obtained causality factors (*CF*2 and *CF*3) are

very closed to the theoretical values (2 and 3) which revealed that the measured data are of high quality [21, 26].

Table 5. Electrochemical frequency modulation parameters for P22 steel in 1 M HCl in the absence and presence of 1.5 g·L^{-1} of CC with different degreasing stages.

Inhibitor	i_{corr}^{EFM} (μA·cm^{-2})	β_a (mV·dec^{-1})	β_c (mV·dec^{-1})	IE_{EFM} (%)	$CI_{95\%}$	*CF* (2)	*CF* (3)
Blank	1211.1±73.5	67.4±1.5	86.7±2.9	Blank	Blank	1.94±0.05	3.12±0.29
CC-0	205.6±6.7	70.3±0.4	116.4±5.3	83.0±0.6	(82.6; 83.4)	1.96±0.02	3.23±0.15
CC-1	226.8±4.4	70.0±1.2	127.2±3.1	81.3±0.4	(80.9; 81.7)	1.96±0.01	3.10±0.63
CC-2	219.1±5.6	62.9±8.6	120.2±2.9	81.9±0.5	(81.5; 82.3)	1.91±0.06	2.90±0.15

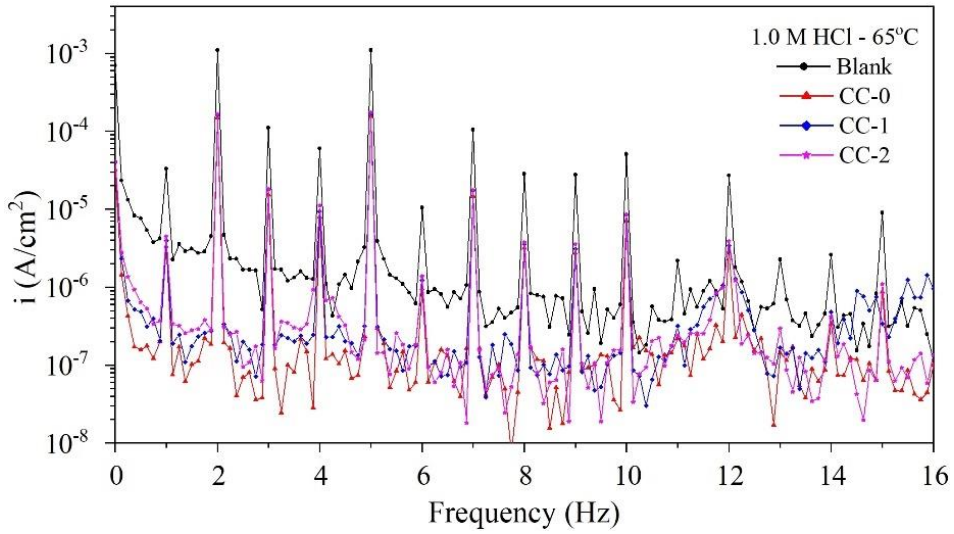

Figure 7. Effect of the type of CC, with a dosage of 1.5 g·L^{-1}, on the intermodulation spectra of P22 steel in 1.0 M HCl at 65°C.

Electrochemical Impedance Spectroscopy measurements

EIS measurements can been used to study the kinetics of the electrochemical processes and the effect of CIs on the electric double layer properties of the metal surface in acidic media. Figure 8 display the Nyquist, Bode phase and Bode modulus plots of the EIS results obtained during the corrosion of P22 steel in 1 M HCl at 65°C, in the absence and presence of 1.5 g·L^{-1} of the CC obtained with the different degreasing stages. Impedance spectra presents a single capacitive loop: this indicates that the corrosion of P22 steel in HCl at 65°C mainly involves the single charger transfer process during the corrosion processes. Analogous shapes of the Nyquist plots without and with CC indicates that inhibitor does not change the mechanism of acidic corrosion. As can be seen in Figure 8a, the Nyquist plot diameter considerably increased with CC and is considered as an indicator of the strength of CIs in inhibiting the corrosion process. Figure 8b shows that the phase angle peaks in the

presence of CC are broader than in the uninhibited system indicating the adsorption of the inhibitor on the metal surface [29]. Furthermore, the absolute impedance values at low frequency in the presence of CC are higher than in the blank system, which confirms the protection of the steel due to the inhibitor adsorption on the metallic surface. The electrochemical parameters collected from fitting the impedance data to the modified Randles equivalent circuit are listed in Table 4. As can be seen from Table 6, the value of charge transfer resistance (R_{ct}) increases, while the value the double-layer capacitance (C_{dl}) decreases in the presence of CC inhibitors. These results suggest that carrageenan molecules have been absorbed onto the steel surface and formed a protective barrier which can hinder the charge and mass transfer. The decrease in C_{dl} values can be attributed to the decrease in local dielectric constant and/or the increase in the thickness of the electrical double layer, due to the replacement of small water molecules by the large carrageenan molecules. Moreover, the number of CC-0 molecules absorbed onto steel surface increases in the presence of KCl and NaCl [27, 28], and the inhibition efficiency increases accordingly. The CC-0 generates the highest inhibition efficiency (%IE_{EIS}=85.5) compared to CC-1 and CC-2; this is statistically confirmed in the ANOVA analysis realized and corroborate what was obtained with the other applied techniques.

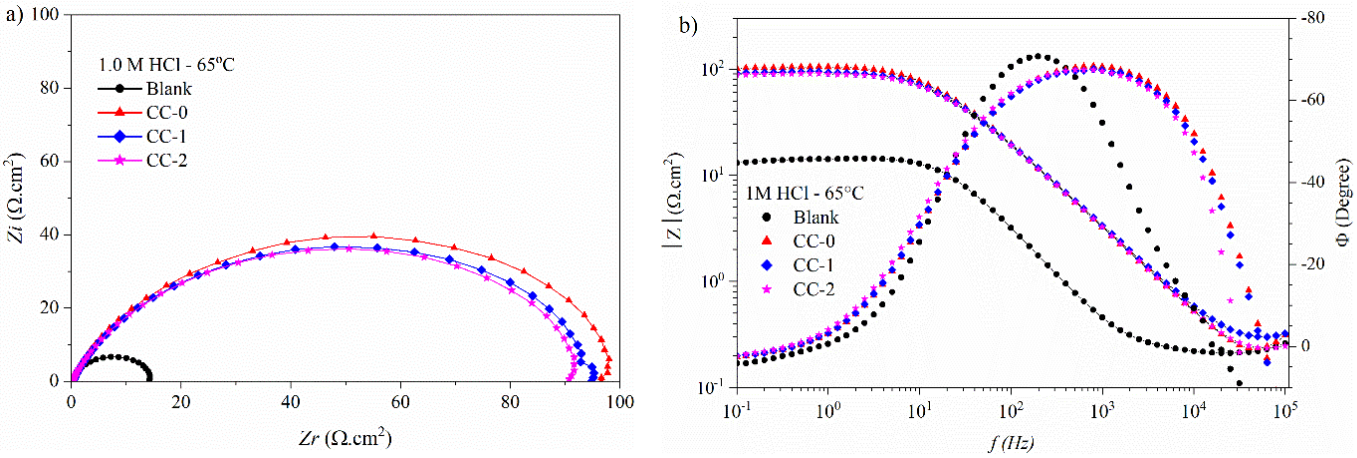

Figure 8. Effect of the type of CC, with a dosage of 1.5 g·L^{-1}, on the impedance spectra of P22 steel in 1 M HCl at 65°C.

Table 6. EIS parameters for P22 steel in 1 M HCl at 65°C, in the absence and presence of 1.5 g·L^{-1} of CC with different degreasing stages.

Inhibitors	R_s (Ω·cm^2)	R_{ct} (Ω·cm^2)	C_{dl} (μF·cm^{-2})	V_{corr}^{EIS} (mm·year^{-1})	IE_{EIS} (%)	$CI_{95\%}$	n
Blank	0.24±0.02	14.2±0.4	525.3±64	13.47±0.39	Blank	Blank	0.952
CC-0	0.22±0.03	98.2±3.1	90.9±6.3	2.25±0.07	85.5±0.4	(85.0; 86.1)	0.861
CC-1	0.24±0.09	91.7±2.8	96.9±7.0	2.49±0.08	84.5±0.5	(83.9; 85.1)	0.856
CC-2	0.26±0.05	88.7±4.6	105.0±7.8	2.35±0.12	83.9±0.8	(83.4; 84.5)	0.855

3.2. Carrageenan obtained at 80°C with different degrease stages

3.2.1. Hot carrageenan Yield

Table 7 shows the statistical results of the ANOVA and the results of Dunnett's multiple comparison test of the hot carrageenan extraction yield (EY_{HC}), obtained as a function of the degreasing stages applied in the extraction tests. As can be seen from Table 7, the $CI_{95\%}$ of the extraction yield mean of HC-0 does not overlap with the $CI_{95\%}$ of the HC-1 and HC-2, which indicate that is significantly different. In the case of HC-1 and HC-2, their $CI_{95\%}$ overlap, indicating that there is no significant difference between the yields results obtained. Dunnett's method of multiple comparisons determined that degreasing generates a higher EY_{HC}, being only necessary one degrease. The *p*-values of the *t*-Student test are less than 0.05, establishing a statistically significant difference between the means of the EY_{HC} without and with degrease stages, with a confidence level of 97.32%.

Table 7. Statistical results of the ANOVA and Dunnett's multiple comparison tests for the extraction yield of HC with different degreasing stages.

Degreasing stages	**N**	**Mean**	**Std Deviation**	$CI_{95\%}$
0	10	24.477	0.830	(23.691–25.263)
1	7	28.704	1.046	(27.764–29.644)
2	7	28.959	1.696	(28.019–29.899)

Level difference	**Mean difference**	**Std Error of difference**	$CI_{95\%}$	***t*-value**	***p*-value**
1–0	4.227	0.589	(2.824; 5.631)	7.17	0.000
2–0	4.482	0.589	(3.078; 5.885)	7.60	0.000

3.2.2. Hot carrageenan characterization

The X-ray diffraction patterns of the HC, obtained with different degreasing stages are shown in Figure 9. XRD patterns analysis of the HC showed no characteristic sharp peaks, indicated that the HC is amorphous in nature. Similar patterns were observed in other types of polysaccharides [30]. Temperature probably affects the crystalline ordering of sulfates in carrageenan and the presence of the characteristic peaks of $K_3Na(SO_4)_2$ is not observed.

Figure 10 shows the SEM image of the HC without degreasing (HC-0) together with the EDS spectrum corresponding to the total mapping of the HC-0 analyzed in said image. Comparing the EDS spectrums of the CC-0 and HC-0 (Figure 10 and 3), it is observed that HC-0 has a lower concentration of Cl, which agrees with the XRD analysis that did not detect the KCl and NaCl phases. A higher content of S and O is also observed in HC-0, which is probably due to a higher content of carrageenan in the sample.

Figure 11 shows the FTIR spectrums of the HC obtained without and with 1 and 2 degreasing stages. The three spectrums are very similar and show intense bands at 1230–1260 cm^{-1}, indicative of the existence of a sulphate ester and corresponding to S=O bonds [22]. Bands at 1072 cm^{-1} and 930 cm^{-1}, both corresponding to the C–O bond of

3,6-anhydrogalactose [22]. The peaks at 845 and 805 cm^{-1} suggested the presence the C–O–SO_4 on C_4 of galactose and C–O–SO_4 on C_2 of 3,6-anhydrogalactose, respectively [22, 23]. Therefore, the structural character of HC is a mixture of κ/ι-carrageenan. The comparison of the FTIR spectrum of the carrageenans obtained at 25°C (Figure 4) and 80°C (Figure 11), shows that the main difference observed concerns the characteristic bands at 614 cm^{-1}, 1100 cm^{-1} and 1191 cm^{-1} corresponding to $K_3Na(SO_4)_2$, which are not observed in HC. Also, the content of κ-carrageenan and ι-carrageenan is higher in HC, which is visualized by the greater intensity of the 930 cm^{-1}, 845 cm^{-1} and 805 cm^{-1} bands.

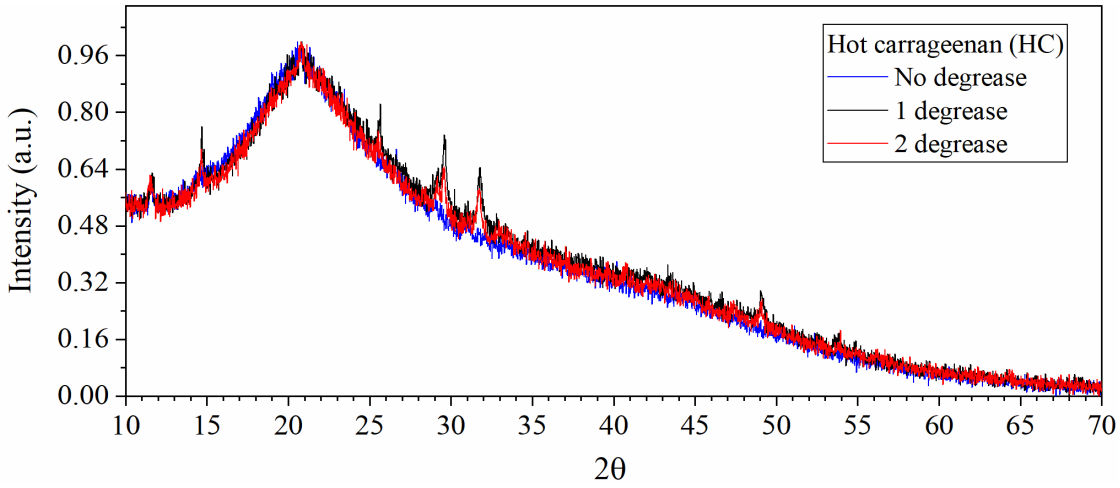

Figure 9. X-ray diffraction pattern of carrageenans obtained at 80°C with different degreasing stage.

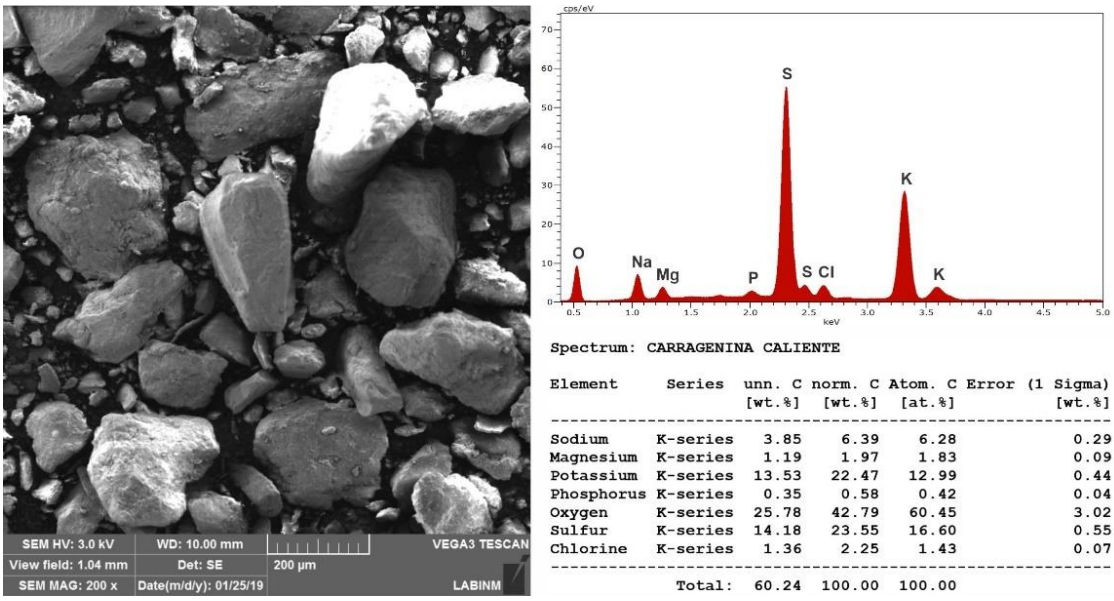

Spectrum: CARRAGENINA CALIENTE

Element	Series	unn. C [wt.%]	norm. C [wt.%]	Atom. C [at.%]	Error (1 Sigma) [wt.%]
Sodium	K-series	3.85	6.39	6.28	0.29
Magnesium	K-series	1.19	1.97	1.83	0.09
Potassium	K-series	13.53	22.47	12.99	0.44
Phosphorus	K-series	0.35	0.58	0.42	0.04
Oxygen	K-series	25.78	42.79	60.45	3.02
Sulfur	K-series	14.18	23.55	16.60	0.55
Chlorine	K-series	1.36	2.25	1.43	0.07
	Total:	60.24	100.00	100.00	

Figure 10. SEM image and total EDS spectrum of carrageenan obtained at 80°C without degrease (HC-0).

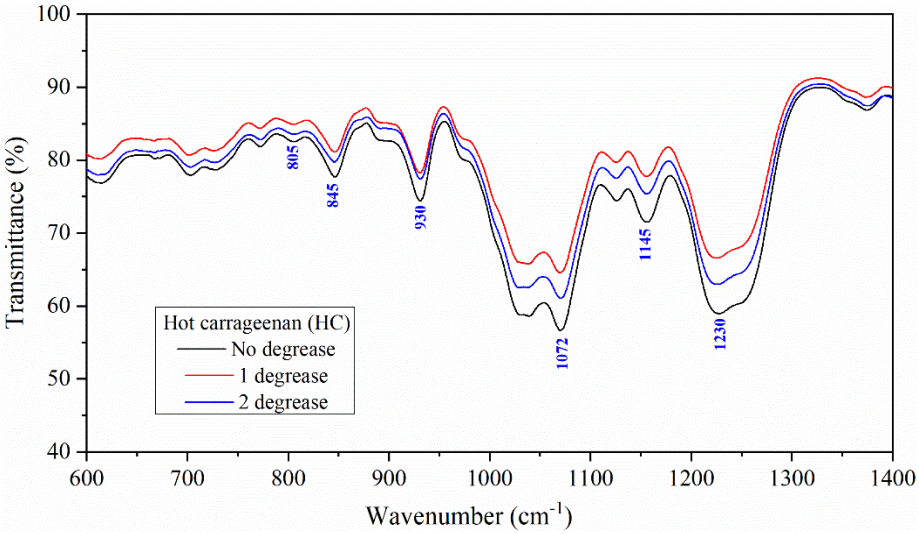

Figure 11. FTIR spectrums of carrageenan obtained at 80°C with different degreasing stages.

3.2.3. Corrosion inhibition efficiency of hot carrageenan

To evaluate the inhibitory effect of the corrosion of the HC, the same techniques used in the CC were used.

Gravimetric measurements

Table 8 shows the results of the weight loss tests of P22 steel in 1 M HCl at 65°C, without and with 1.5 g·L^{-1} of HC obtained with different degreasing stages. It is observed that the IE_c of the three hot carrageenans are relatively high. This finding can be explained by the adsorption of carrageenan molecules on the surface of P22 steel. This occurs via a partial sharing of the electrons from the unprotonated oxygen atoms and $-OSO^{3-}$ atoms with the anodic sites of the metal surface. The vacant d orbitals of Fe^{2+} ions receive the shared electrons and anodic metal dissolution will be inhibited [31]. The ANOVA reported an overlap of the $CI_{95\%}$ of the corrosion inhibition efficiency means (IE_{WL}) of the three HC, which indicates that they are not significantly different.

Table 8. Weight loss results of P22 steel in 1 M HCl at 65°C, in the absence and presence of 1.5 g·L^{-1} of HC with different degreasing stages.

Inhibitor	V_{corr}^{WL} (mm·year^{-1})	$\%IE_{WL}$	$CI_{95\%}$
Blank	26.97±0.43	Blank	Blank
HC-0	3.36±0.34	87.56±1.26	(86.37; 88.74)
HC-1	3.68±0.23	86.35±0.86	(84.98; 87.72)
HC-2	3.41±0.23	87.35±0.87	(86.16; 88.54)

Potentiodynamic polarization measurements

The polarization curves of the P22 steel in 1 M HCl at 65°C without and with 1.5 g·L^{-1} HC obtained with different degreasing stages are shown in Figure 12. The Table 9 lists the relevant electrochemical parameters, including corrosion potential (E_{corr}), corrosion current density (i_{corr}^{PDP}), anodic and cathodic Tafel slope (β_a, β_c), and inhibition efficiency (IE_{PDP}), which were obtained from the polarization curves. As can be seen in Figure 12, both anodic and cathodic curves move to the direction of low current density after adding HC. This consequence is consistent with the decreasing of the i_{corr}^{PDP} values and the increasing of the IE_{PDP} values (Table 9). The phenomenon suggested that both anodic steel dissolution and cathodic hydrogen evolution were retarded by HC. Besides, the little change in E_{corr} indicated that HC can be considered a mixed-type inhibitor with a predominant control of the anodic reaction [29]. The ANOVA test performed shows an overlap of the $CI_{95\%}$ of the inhibition efficiency means (IE_{PDP}) obtained with the three HC, so they are not significantly different. This confirms the results obtained in the gravimetric tests.

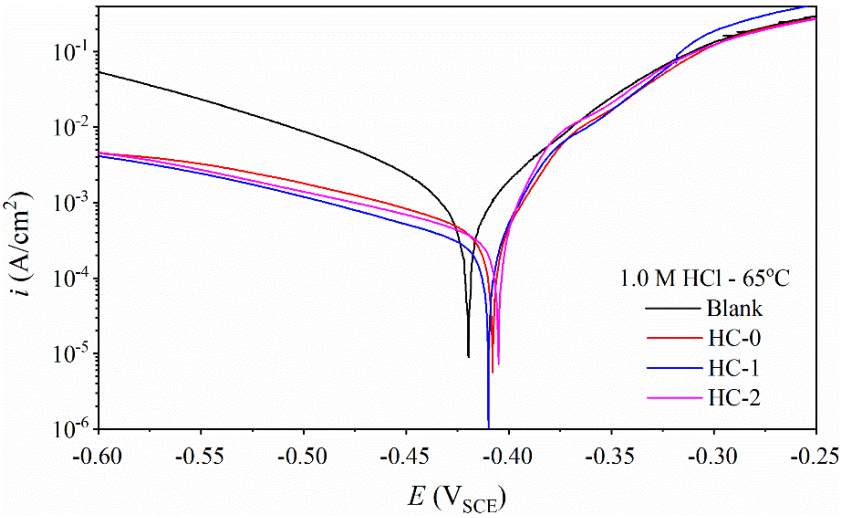

Figure 12. Effect of the type of HC, with a concentration of 1.5 g·L^{-1}, on the potentiodynamic curves of P22 steel in 1 M HCl at 65°C.

Table 9. Polarization curve parameters of P22 steel in 1 M HCl at 65°C without and with 1.5 g·L^{-1} of HC with different degreasing stages.

Inhibitor	i_{corr}^{PDP} **(μA·cm^{-2})**	$-E_{corr}$ **(mV *vs.* SCE)**	β_a **(mV·dec^{-1})**	β_c **(mV·dec^{-1})**	IE_{PDP} **(%)**	$CI_{95\%}$
Blank	2058.2±142.2	420.3±0.8	65.2±2.6	127.6±2.3	Blank	Blank
HC-0	361.6±61.8	409.5±1.7	26.4±0.8	171.7±4.7	82.4±3.0	(78.31; 86.54)
HC-1	334.3±71.4	410.3±1.1	29.6±1.3	174.7±8.3	83.8±3.5	(79.64; 87.88)
HC-2	342.0±43.2	404.7±0.6	27.4±3.5	174.7±11.3	83.4±2.1	(79.26; 87.50)

Linear polarization resistance measurements

LPR plots for P22 steel in 1 M HCl without and with 1.5 g·L^{-1} of HC obtained with different degreasing stages are shown in Figure 13. The values of the polarization resistance (R_p) obtained from linear polarization resistance (LPR) tests are listed in Table 10. It is observed that R_p increases with the hot carrageenan and reaches a maximum of about 70 Ω·cm^2 with the addition of 1.5 g·L^{-1} of HC, compared as the 14.8 Ω·cm^2 for the blank solution. The increase in polarization resistance in the presence of HC suggests that a non-conducting physical barrier is formed at metal/electrolyte interface. The ANOVA reported an overlap of the $CI_{95\%}$ of the inhibition efficiency means (IE_{Rp}) of the three HC, which indicates that they are not significantly different. This confirms the results obtained with the other techniques.

Table 10. Results of polarization resistance tests for corrosion of P22 steel in 1 M HCl at 65°C without and with 1.5 g·L^{-1} of HC with different degreasing stages.

Inhibitor	R_p (Ω·cm^2)	V_{corr}^{EIS} (mm·year^{-1})	IE_{Rp} (%)	$CI_{95\%}$
Blank	14.87±0.51	12.87±0.44	Blank	Blank
HC-0	69.56±2.72	3.22±0.13	78.6±0.8	(77.82; 79.38)
HC-1	69.47±2.66	3.21±0.12	78.6±0.8	(77.80; 79.36)
HC-2	71.38±3.77	3.10±0.16	79.13±1.1	(78.27; 79.98)

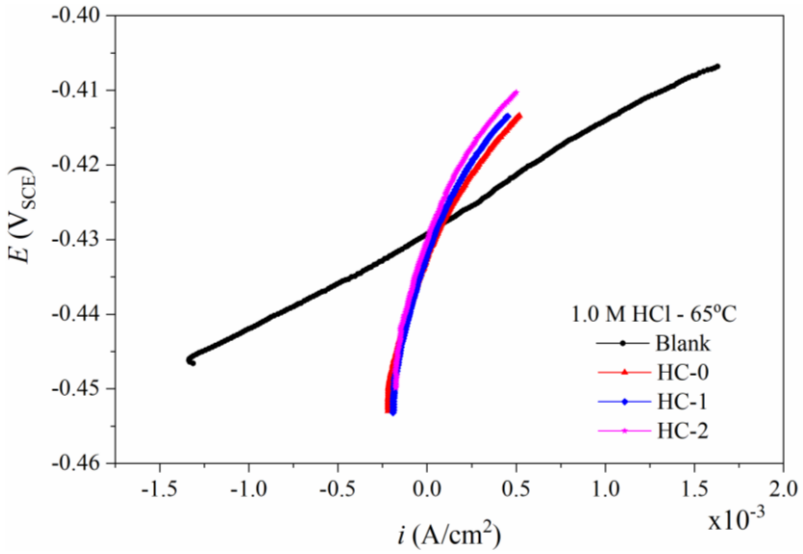

Figure 13. Effect of the type of HC, with a concentration of 1.5 g·L^{-1}, on the linear polarization resistance curves of P22 steel in 1 M HCl at 65°C.

Electrochemical frequency modulation measurements

The EFM technique was used to calculate the corrosion current densities as well as the anodic and cathodic Tafel slopes for the P22 steel in a 1 M HCl solution at 65°C, without

and with a concentration of 1.5 g·L^{-1} of the three types of HC. Figure 12 shows a representative intermodulation spectrum of each evaluated HC. The calculated electrochemical parameters (i_{corr}^{EFM}, β_a, β_c, *CF*(2), *CF*(3) and %IE_{EFM}) are given in Table 11. Inspections of these data infer that the values of causality factors obtained are approximately equal the theoretical values 2 and 3, indicating that the measured data are of high quality [21, 26]. In agreement with the other techniques used, the EFM tests show that the IE_c of the three carrageenans are statistically similar: about 79%. This is concluded due to the superposition of the $CI_{95\%}$ of the inhibition efficiency means. The degrease stage does not produce a change in the anticorrosive strength of the HC.

Table 11. Electrochemical frequency modulation parameters for P22 steel in 1 M HCl in the absence and presence of 1.5 g·L^{-1} HC with different degreasing stages.

Inhibitor	i_{corr}^{EFM} **(μA·cm^{-2})**	β_a **(mV·dec^{-1})**	β_c **(mV·dec^{-1})**	**%IE_{EFM}**	***CI*$_{95\%}$**	***CF*(2)**	***CF*(3)**
Blank	1211.1±73.5	67.4±1.5	86.7±2.9	Blank	Blank	1.94±0.05	3.12±0.29
HC-0	251.8±10.1	69.0±1.0	124.8±2.3	79.2±0.8	(78.4; 80.0)	1.96±0.01	3.05±0.24
HC-1	250.5±14.7	69.2±1.0	121.8±1.9	79.3±1.2	(78.5; 80.1)	1.94±0.02	3.07±0.09
HC-2	238.7±8.3	68.4±1.5	121.7±3.6	80.3±0.7	(79.5; 81.1)	1.95±0.04	3.12±0.21

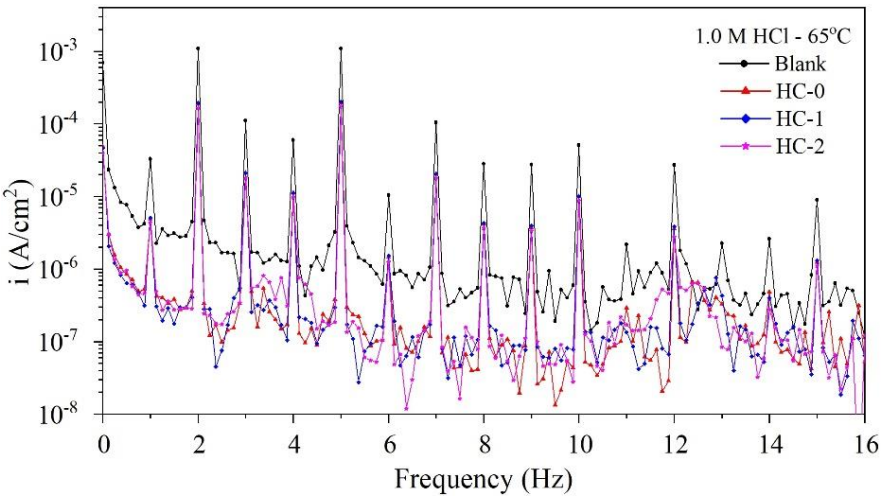

Figure 14. Effect of the type of HC, with a concentration of 1.5 g·L^{-1}, on the intermodulation spectra of P22 steel in 1 M HCl at 65°C.

Electrochemical impedance spectroscopy measurements

The EIS data for P22 steel in 1 M HCl at 65°C, without and with a concentration of 1.5 g·L^{-1} of the three types of HC are presented as Nyquist, Bode phase angle, and Bode modulus plots in Figure 15. The Nyquist plots, have depressed capacitive semicircles, indicating that the corrosion and corrosion inhibition processes are under charge transfer

control. As seen in Figure 15a, the Nyquist plots with HC in solution have a large diameter with respect to the blank. This can be related to the anticorrosive action of HC, which enhances the resistance of the P22 steel surface to corrosion. Figure 15b elucidated broader peaks in the presence of HC indicating a relaxation effect due to the formation of a barrier layer on the steel surface [29]. Moreover, the values of log|*Z*| improved considerably at low frequencies in the presence of HC. The parameters obtained in the EIS tests are shown in Table 12. The presence of HC in the corrosive medium produces an increase in R_{ct} and a decrease in C_{dl}. This suggests that the adsorption of carrageenan molecules on the surface of the steel hinders the charge transfer process due to the increase in the thickness of the electrical double layer. In addition, the adsorbed molecules decrease the dielectric constant of the electrical double layer and therefore its capacitance. The ANOVA confirms what was obtained with the other applied techniques; that is, degrease does not statistically modify the IE_c of the HC, being its inhibition efficiency of about 83%.

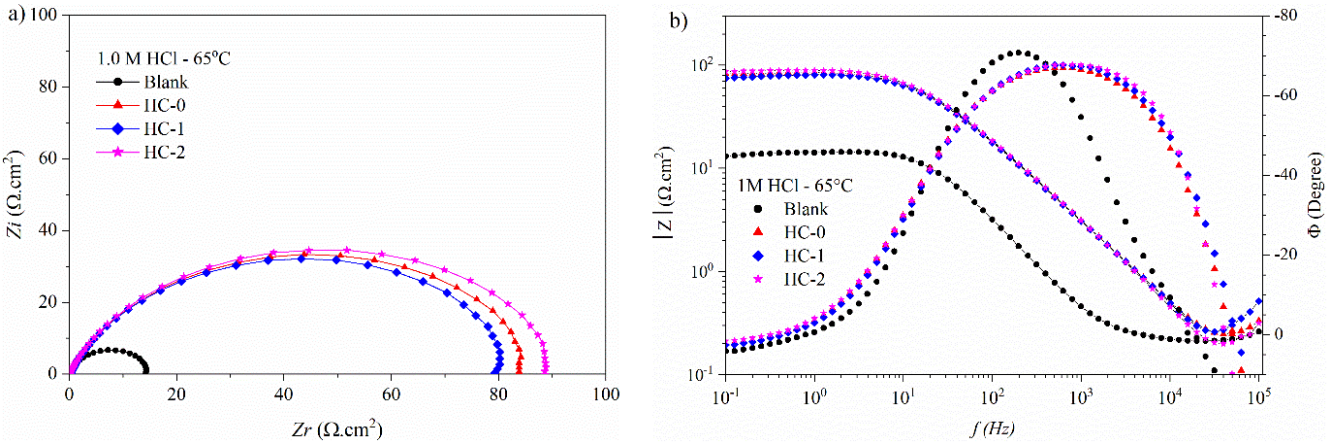

Figure 15. Effect of the type of HC, with a dosage of 1.5 g·L^{-1}, on the Nyquist diagrams of P22 steel in 1 M HCl at 65°C.

Table 12. EIS parameters for P22 steel in 1 M HCl at 65°C, in the absence and presence of 1.5 g·L^{-1} of HC with different degreasing stages.

Inhibitors	R_s (Ω·cm^2)	R_{ct} (Ω·cm^2)	C_{dl} (μF·cm^{-2})	V_{corr}^{EIS} (mm·year^{-1})	IE_{EIS} (%)	$CI_{95\%}$	n
Blank	0.24±0.02	14.2±0.4	525.3±64	13.47±0.39	Blank	Blank	0.952
HC-0	0.28±0.04	81.5±2.4	106.9±4.6	2.75±0.08	82.6±0.5	(81.8; 83.3)	0.857
HC-1	0.24±0.04	83.2±5.6	101.5±4.3	2.68±0.18	82.9±1.2	(82.1; 83.6)	0.861
HC-2	0.25±0.05	85.8±4.5	103.2±3.9	2.58±0.13	83.4±0.8	(82.6; 84.2)	0.871

3.3 Analysis of the corrosion inhibition efficiency with the carrageenans obtained

Table 13 summarizes the inhibition efficiency values obtained with the five techniques used in the evaluation of the corrosion of P22 steel in 1 M HCl at 65°C, in the presence of

1.5 $g \cdot L^{-1}$ of carrageenan. The six carrageenans obtained with the different extraction processes showed good corrosion inhibition efficiency. Cold carrageenan without the degreasing stage (CC-0) has a relatively higher inhibition efficiency. This is probably due to the synergistic effect of chloride ions, which enhance the adsorption capacity of organic inhibitor on the metal surface [27, 28]. The degreasing stage reduces the inhibition efficiency of the CC, but does not affect the inhibition efficiency of the HC. Corrosion inhibition efficiency results obtained with each of the five techniques used for each evaluated carrageenan showed excellent agreement. Based in the results obtained in this study, the recommended extraction process would be the extraction of CC and HC without degrease in the same extraction process, which allows to obtain an extraction yield of around the 45.9% (CC: 21.4±0.8; HC: 24.5±0.8), and with a high inhibition efficiency. This extraction yield agrees with what was reported in the reference [32].

Table 13. Corrosion inhibition efficiency of P22 steel in 1 M HCl at 65°C, obtained with a concentration of 1.5 $g \cdot L^{-1}$ of each of the evaluated carrageenans.

Carrageenan	Inhibition efficiency (%)				
	WL	**PDP**	**EFM**	**EIS**	**LPR**
CF-0	88.2±0.5	91.1±0.7	83.0±0.6	85.5±0.4	82.6±0.6
CF-1	86.8±0.4	84.1±0.6	81.3±0.4	84.5±0.5	79.6±0.6
CF-2	86.5±0.2	84.0±1.0	81.9±0.5	83.9±0.8	79.7±1.1
CC-0	87.6±1.2	90.5±0.6	79.2±0.8	82.6±0.5	78.3±0.8
CC-1	86.3±0.9	90.8±1.1	78.8±0.9	81.7±1.2	78.3±0.8
CC-2	87.3±0.9	87.6±1.9	80.1±0.7	83.4±0.8	78.4±1.4

4. Conclusions

This study demonstrates that carrageenan can be extracted with a simple and inexpensive method and used as a green inhibitor in chemical cleaning processes of steels with HCl. The main conclusions were drawn as follows:

1. Cold carrageenan (CC) is mainly composed of κ-carrageenan in the presence of KCl, NaCl and $K_3Na(SO_4)_2$. The degreasing stage reduces the KCl and NaCl content in the CC. Hot carragenan has an amorphous structure composed of a mixture of κ-carrageenan and ι-carrageenan.
2. The highest extraction yield (*EY*) of the CC was 21.43% and was obtained without the degreasing stage (CC-0); while the highest extraction yield of the HC was 28.96% and was obtained with 2 degreasing stages (HC-2).
3. The six carrageenans obtained with the different extraction processes show good corrosion inhibition efficiency. However, CC without degreasing (CC-1) presents the highest

inhibition efficiency, 85.5% (EIS technique). The degreasing process does not significantly affect the inhibition efficiency of the HC, it was about 82.0 (EIS technique).

4. Corrosion inhibition efficiency results obtained with each of the five techniques used for each evaluated carrageenan showed excellent agreement
5. Based in the results obtained in this study, the recommended extraction process would be the extraction of CC-1 and HC-1 in the same extraction process, obtaining a semi-refined, economical carrageenan, with an extraction yield of about 45.9% and with a high inhibition efficiency.

Acknowledgements

This project was financed by the National Council of Science, Technology and Technological Innovation – CONCYTEC according to agreement 120-2015-FONDECYT-DE.

Reference

1. H. Baorong, *The Cost of Corrosion in China*, Science Press, Bejing, 2018, 33.
2. R.T. Carvalho, P.F. Oliveira, L.C. Palermo, A.A. Ferreira and C.R. Mansur, Prospective acid microemulsions development for matrix acidizing petroleum reservoirs, *Fuel*, 2019, **238**, 75–85. doi: 10.1016/j.fuel.2018.10.003
3. E. Ituen, O. Akaranta and A. James, Evaluation of performance of corrosion inhibitors using adsorption isotherm models: An overview, *Chem. Sci. Int. J.*, 2017, **18**, no. 1, 1–34. doi: 10.9734/CSJI/2017/28976
4. J. Arockia Selvi, M. Arthanareeswari, T. Pushpamalini, S. Rajendran and T. Vignesh, Effectiveness of *Vinca rosea* leaf extract as corrosion inhibitor for mild steel in 1 N HCl medium investigated by adsorption and electrochemical studies, *Int. J. Corros. Scale Inhib*., 2020, **9**, no. 4, 1429–1443. doi: 10.17675/2305-6894-2020-9-4-15
5. M.A. Quraishi, D.S. Chauhan and V.S. Saji, *Heterocyclic Organic Corrosion Inhibitors: Principles and applications*, Elsevier, 2020. doi: 10.1016/C2018-0-04237-1
6. S. Rajendran, R. Srinivasan, R. Dorothy, T. Umasankareswari and A. Al-Hashem, Green solution to corrosion problems – at a glance, *Int. J. Corros. Scale Inhib*., 2019, **8**, no. 3, 437–479. doi: 10.17675/2305-6894-2019-8-3-1
7. M. Finsgar and J. Jackson, Application of corrosion inhibitors for steels in acidic media for the oil and gas industry: A review, *Corros. Sci*., 2014, **86**, 17–41. doi: 10.1016/j.corsci.2014.04.044
8. S.K. Sharma, Chapter 6 – Green corrosion chemistry and engineering, *Green Corrosion Chemistry and Engineering: Opportunities and Challenges*, Wiley-VCH Verlag GmbH & Co, 2011, 157–180. doi: 10.1002/9783527641789.ch6
9. B.A. Abd-El-Nabey, D.E. Abd-El-Khalek, S. El-Housseiny and M.E. Mohamed, Plant extracts as corrosion and scale inhibitors: A review, *Int. J. Corros. Scale Inhib*., 2020, **9**, no. 4, 1287–1328. doi: 10.17675/2305-6894-2020-9-4-7

10. M. Mobin, I. Ahmad, M. Basik, M. Murmu and P. Banerjee, Experimental and theoretical assessment of almond gum as an economically and environmentally viable corrosion inhibitor for mild steel in 1 M HCl, *Sustainable Chem. Pharm.*, 2020, **18**, 100337. doi: 10.1016/j.scp.2020.100337
11. L. Guo, R. Zhang, B. Tan, W. Li, H. Liu and S. Wu, Locust bean gum as a green and novel corrosion inhibitor for Q235 steel in 0.5 M H_2SO_4 medium, *J. Mol. Liq.*, 2020, **310**, 113–239. doi: 10.1016/j.molliq.2020.113239
12. K.O. Shamsheera, R.P. Anupama and J. Abraham, Computational simulation, surface characterization, adsorption studies and electrochemical investigation on the interaction of guar gum with steel in HCl environment, *Results Chem.*, 2020, **2**, 100054. doi: 10.1016/j.rechem.2020.100054
13. M. Mobin, M. Basik and J. Aslam, *Boswellia serrata* gum as highly efficient and sustainable corrosion inhibitor for low carbon steel in 1 M HCl solution: Experimental and DFT studies, *J. Mol. Liq.*, 2018, **263**, 174–186. doi: 10.1016/j.molliq.2018.04.150
14. M. Mobin, M. Rizvi, L.O. Olasunkanmi and E.E. Ebenso, Biopolymer from tragacanth gum as a green corrosion inhibitor for carbon steel in 1 M HCl solution, *ACS Omega*, 2017, **2**, no. 7, 3997–4008. doi: 10.1021/acsomega.7b00436
15. A. Biswas, S. Pal and G. Udayabhanu, Experimental and theoretical studies of xanthan gum and its graft co-polymer as corrosion inhibitor for mild steel in 15% HCl, *Appl. Surf. Sci.*, 2015, **353**, no. 30, 173–183. doi: 10.1016/j.apsusc.2015.06.128
16. M. Mobin and M. Rizvi, Inhibitory effect of xanthan gum and synergistic surfactant additives for mild steel corrosion in 1 M HCl, *Carbohydr. Polym.*, 2016, **136**, 384–393. doi: 10.1016/j.carbpol.2015.09.027
17. S.A. Umoren, Inhibition of aluminium and mild steel corrosion in acidic medium using gum Arabic, *Cellulose*, 2008, **15**, no. 5, 751–761. doi: 10.1007/s10570-008-9226-4
18. P. Wang, X. Zhao, Y. Lv, M. Li, X. Liu, G. Li and G. Yu, Structural and compositional characteristics of hybrid carrageenans from red algae *Chondracanthus chamissoi*, *Carbohydr. Polym.*, 2012, **89**, no. 3, 914–919. doi: 10.1016/j.carbpol.2012.04.034
19. D. Gandy, *The Grade 22 Low Alloys Steel Handbook*, Electric Power Research Institute, 2005.
20. G. Yu, B. Yang, W. Ren, X. Zhao, J. Zhang and C. Barrow, A comparative analysis of four kinds of polysaccharides purified from *Furcellaria lumbricalis*, *J. Ocean Univ. China*, 2007, **6**, no. 1, 16–20. doi: 10.1007/s11802-007-0016-7
21. R.W. Bosch, J.W. Hubrecht, B.C. Syrett and W.F. Bogaerts, Electrochemical Frequency Modulation: A New Electrochemical Technique for Online Corrosion Monitoring, *Corrosion*, 2001, **57**, no. 1, 60–70. doi: 10.5006/1.3290331
22. T. Chopin, B.F. Kerin and R. Mazerolle, Phycocolloid chemistry as a taxonomic indicator of phylogeny in the Gigartinales, Rhodophyceae: A review and current developments using Fourier transform infrared diffuse reflectance spectroscopy, *Phycol. Res.*, 1999, **47**, no. 3, 167–188.

23. L. Pereira, A.M. Amado, A.T. Critchley, F. Van de Velde and P.J.A. Ribeiro-Claro, Identification of selected seaweed polysaccharides (phycocolloids) by vibrational spectroscopy (FTIR-ATR and FT-Raman), *Food Hydrocolloids*, 2009, **23**, no. 7, 1903–1909. doi: 10.1016/j.foodhyd.2008.11.014
24. A. Choubey, S. Das, S.K. Sharma and J. Manam, Calculation for the trapping parameters of $K_3Na(SO_4)_2$ phosphor by isothermal luminescence decay method, *Mater. Chem. Phys*., 2010, **120**, no. 2–3, 472–475. doi: 10.1016/j.matchemphys.2009.11.038
25. S.A. Umoren and M.M. Solomon, Effect of halide ions on the corrosion inhibition efficiency of different organic species – A review, *J. Ind. Eng. Chem*., 2015, **21**, 81–100. doi: 10.1016/j.jiec.2014.09.033
26. E. Berdimurodov, A. Kholikov, K. Akbarov, L. Guo, A.M. Abdullah and M. Elik, A gossypol derivative as an efficient corrosion inhibitor for St2 steel in 1 M HCl+1 M KCl: An experimental and theoretical investigation, *J. Mol. Liq*., 2021, **328**, no. 1, 115475. doi: 10.1016/j.molliq.2021.115475
27. H.M. Abd El-Lateef and M.M. Khalaf, Synergistic inhibition effect of novel counterion-coupled surfactant based on rice bran oil and halide ion on the C-steel corrosion in molar sulphuric acid: Experimental and computational approaches, *J. Mol. Liq*., 2021, **331**, 115797. doi: 10.1016/j.molliq.2021.115797
28. Z. Yang, Ch. Qian, W. Chen, M. Ding, Y. Wang, F. Zhan and M.U. Tahir, Synergistic effect of the bromide and chloride ion on the inhibition of quaternary ammonium salts in haloid acid, corrosion inhibition of carbon steel measured by weight loss, *Colloid Interface Sci. Commun*., 2020, **34**, 100228. doi: 10.1016/j.colcom.2019.100228
29. A. Thomas, M. Prajila, K.M. Shainy and A. Joseph, A green approach to corrosion inhibition of mild steel in hydrochloric acid using fruit rind extract of *Garcinia indica* (Binda), *J. Mol. Liq*., 2020, **312**, 113369. doi: 10.1016/j.molliq.2020.113369
30. S. Singh and S.B. Bothara, Morphological, physico-chemical and structural characterization of mucilage isolated from seeds of Buchanania lanzan spreng, *Int. J. Health & Allied Sci*., 2014, **3**, no. 1, 33–39. doi: 10.4103/2278-344X.130609
31. N.D. Gowraraju, S. Jagadeesan, K. Ayyasamy, L.O. Olasunkanmi, E.E. Ebenso and C. Subramanian, Adsorption characteristics of Iota-carrageenan and Inulin biopolymers as potential corrosion inhibitors at mild steel/sulphuric acid interface, *J. Mol. Liq*., 2017, **232**, 9–19. doi: 10.1016/j.molliq.2017.02.054
32. K. Véliz, N. Chandía, M. Rivadeneira and M. Thiel, Seasonal variation of carrageenans from *Chondracanthus chamissoi* with a review of variation in the carrageenan contents produced by Gigartinales, *J. Appl. Phycol*., 2017, **29**, 3139–3150. doi: 10.1007/s10811-017-1203-6

♦♦♦